Multi-region Competitive Tractography via Graph-based Random Walks

Brian G. Booth and Ghassan Hamarneh
Medical Image Analysis Lab, School of Computing Science
Simon Fraser University
{bgb2, hamarneh}@sfu.ca

Abstract

We propose a multi-region approach to tractography that not only allows for competition between seed regions, but also allows for the incorporation of knowledge beyond a local scale. By formulating tractography as a graph-based random walk, we are able to obtain a closed-form solution for connection probabilities. Results on synthetic data and thirty images from the MIDAS database show that the introduction of competition reduces erroneous connectivity to regions outside the seeded tracts.

1. Introduction

Diffusion magnetic resonance imaging (dMRI) provides us with the ability to non-invasively assess the integrity and neural connectivity of the brain's white matter. The connectivity is inferred from the measured local diffusion of water molecules, where diffusion rates are known to be maximal along the direction of the underlying axons [2].

The innovation of dMRI has led to the ability to perform tractography: the delineation of neural connections in the brain. Initial streamline approaches gave us the ability to visualize these connections by generating 3D space curves tangent to the direction of maximal local diffusion [1, 15]. These initial methods were limited in that they did not consider the effects of noise, partial voluming, or other imaging artifacts. The streamlines are also formed independently of each other, making it impossible for them to adjust to the position of neighbouring tracts. Further, the streamlines grow based on local information; only the local diffusion profile and the current curvature of the streamline are used to determine its immediate next growth step. This combination of local decision-making, independent curve formation, and disregard of possible errors in the diffusion measurements, can lead streamlines off the path of the underlying neuronal fibers, resulting in a phenomenon known as tract jumping [16].

Later tractography algorithms attempted to address these concerns in various ways. Probabilistic tractography methods use a Monte Carlo generation of streamline curves where the streamlines grow based on a noise model [3, 9]. Approaches involving diffusion simulation have also been proposed[6, 13]. These methods simulate diffusion in a local neighbourhood and use the resulting diffusion front, along with various heuristics, to discover the underlying fiber tracts. Minimal path-based approaches have also been proposed based on Dijkstra's algorithm [12, 20]. While these advancements consider the effects of noise in different ways, these algorithm still generate tracts in a local and greedy fashion. Any information we wish to incorporate into tractography algorithms is currently limited to a local scale (*e.g.,* fractional anisotropy, local tract curvature). Even recent global tractography algorithms continue to be driven solely by local tract properties (*e.g.,* [8]). All these methods also generate, for different fiber tracts, estimates that are independent of each other's locations, thus overlooking the fact that these tracts exist in the same spatial domain and affect each other's position.

To improve the robustness of tractography algorithms, we must address the aspects of tractography algorithms that limit their effectiveness: locally-driven decision making and independent tract formation. With these characteristics in mind, we propose a novel approach to tractography by incorporating the notion of *competition*. At a high level, we propose a tractography algorithm where tracts compete for space within the brain. This competition is introduced using multiple seed regions in a graph-based random walk framework [11]. The steps of the random walker are driven by the dMRI data so that the walker's trajectory aligns with the underlying neural pathways. In this framework, we compute the probability that a random walker will reach a particular seed region *first*. The temporal aspect of this random walk encodes the notion of competition into the tractography process. The connection probabilities are then computed as a closed-form solution that explicitly incorporates the effects of multiple seed regions.

We present our tractography algorithm in the following section and apply the algorithm to both synthetic data and 30 diffusion MR images from the MIDAS database [5]. Results show that introducing competition allows us to reduce erroneous connectivity while also reducing the effect local noise has on the resulting connection probabilities.

2. Methods

We begin by stating the problem formally. Let $\mathcal{I} : \Omega \to \mathcal{M}$ be a diffusion volume that maps a point $\mathbf{x}$ in the image space Ω to a fiber orientation distribution function (fODF) $\phi_{\mathbf{x}} \in \mathcal{M}$. The fODFs can be computed using any one of many methods (*e.g.,* [7]) as long as $\phi_{\mathbf{x}}$ is a point on the manifold $\mathcal{M}$ of allowable fiber ODFs.

We consider a point $\mathbf{x}$ and its relation to a set of seed regions $\Psi = \{\mathcal{R}_1, \cdots, \mathcal{R}_K\}$ in terms of a random walk problem. Our goal is to determine a mapping

$$z : \Psi \times \mathbf{x} \times \mathcal{I} \to [0,1]^K \tag{1}$$

that would tell us the probabilities of a diffusion MRI driven random walker, originating at a position $\mathbf{x}$, stumbling on a region $\mathcal{R}_k$ before any other region $\mathcal{R}_{k'} \in \Psi \setminus \mathcal{R}_k$. By controlling the random walker using the fODF information, the probabilities we generate are interpreted as connection probabilities in the same way as traditional probabilistic tractography results (*i.e.,* tractograms).

2.1. Graph Construction

We represent a diffusion MR volume as an undirected graph $G = (V, E)$ where the set of nodes V is the set of voxels and $E \subset (V \times V)$ are edges connecting pairs of voxels in the MR volume. As the fODFs captures only local directional diffusion information, we restrict the graph's edges to a voxel's 26 neighbours in 3D.

To guide the random walk on our graph structure, we require transition probabilities between graph nodes. These probabilities are encoded as edge weights in our graph and encapsulate the probability that a neural pathway exists along a particular edge. As in [4], we define the transition probability for an edge e_{ij} as:

$$w(e_{ij}) = p_{wm}(i)p_{wm}(j)\left(\frac{1}{2}\int_\beta \phi_i(\mathbf{r}_{ij}) + \frac{1}{2}\int_\beta \phi_j(\mathbf{r}_{ji})\right) \tag{2}$$

where $p_{wm}(i)$ is the white matter probability at voxel i and $\mathbf{r}_{ij}$ is the unit vector originating at voxel i and pointing towards voxel j. The ODF is integrated over the solid angle $\beta = 4\pi/26$ steradians surrounding the edge so as to fully capture the local diffusion properties [12]. Note that a large edge weight corresponds to both the potential of a neural pathway along the edge as well as a more likely path for the random walker to take.

2.2. Diffusion Simulation

To solve for the probabilities in (1), we use the fact that the solution of the combinatorial Dirichlet problem is equivalent to the solution that we seek [11]. In our context, the Dirichlet problem is essentially to find the probabilities z that minimizes the Dirichlet integral

$$D[z] = \frac{1}{2}\int_\Omega |\nabla z|^2 d\Omega \tag{3}$$

over the diffusion volume Ω. Using our graph representation, we can rewrite (3), as in [11], to be

$$D[z] = \frac{1}{2} z^T L z \tag{4}$$

where L is the Laplacian matrix of the graph. The graph Laplacian is given in [11] as

$$L_{ij} = \begin{cases} d_i & \text{if } i = j, \\ -w_{ij} & \text{if } (i,j) \in E, \\ 0 & \text{otherwise} \end{cases} \tag{5}$$

where w_{ij} is the edge weight for edge e_{ij}, given by (2), and d_i is the degree of node i (the sum of edge weights incident on i).

Once we have the Dirichlet integral set up as in (4), we can differentiate with respect to z and find its critical points. Since L is positive semi-definite, the only critical point of (4) will be the global minimum of (3). This derivation can be found in [11] and leads to a system of linear equations with respect to the given seed regions $\{\mathcal{R}_1, \cdots, \mathcal{R}_K\}$. If we consider, for each region $\mathcal{R}_k$ in turn, a set C_k of nodes within the region, we can define a matrix $M = [\mathbf{m}_1, \cdots, \mathbf{m}_K]$ describing the known probabilities for our seed regions:

$$\mathbf{m}_k(\mathbf{x}) = \begin{cases} 1 & \text{if } \mathbf{x} \in C_k \\ 0 & \text{otherwise.} \end{cases} \tag{6}$$

The resulting linear system of equations takes the form

$$L_u Z_u = -B^T M \tag{7}$$

where our matrix Laplacian from (5) is reordered as

$$L = \begin{bmatrix} L_s & B \\ B^T & L_u \end{bmatrix} \tag{8}$$

Essentially, the Laplacian matrix is ordered so that the nodes within seed regions $\{\mathcal{R}_1, \cdots, \mathcal{R}_K\}$ appear first and the remaining nodes follow. As such, L_u is the Laplacian of the sub-graph excluding regions $\{\mathcal{R}_1, \cdots, \mathcal{R}_K\}$ while B encodes the connectivity between those unseeded nodes and the given seed regions (whose Laplacian is L_s).

The resulting matrix $Z_u = [\mathbf{z}_1, \cdots, \mathbf{z}_K]$ are the connection probabilities for the remaining unseeded nodes. Directly solving (7) for Z_u provides us with the probabilities we seek: the probability a neural connection exists between $\mathbf{x}$ and each seed region. Note that the resulting probabilities from (7) are obtained by matrix inversion and do not require the Monte Carlo sampling seen in [3, 9]. This fact guarantees a repeatable result. For a more detailed version of this derivation, please refer to [11].

2.3. Modelling the Background

Conventional tractography algorithms typically include a termination condition whereby tracking is halted in regions where the fiber direction becomes unclear. This termination condition, typically described by a threshold on fractional anisotropy [1, 3, 9] or local variance in tract direction [15], is used to ensure that the algorithm does not generate fiber tracts where no evidence of coherent axonal tracts exist.

We capture this same tract termination condition by introducing an additional background seed region $\mathcal{R}_{bgnd}$. This region is used to model background regions where the diffusion MRI data is incapable of capturing the underlying axonal fibers. Even with this additional seed region, the interpretation of the probabilities we compute in (7) remains the same. They represent the probability of a random walker reaching a particular seed region before any other seed region *including the background*.

3. Results and Discussion

To examine the properties of our proposed tractography algorithm, we apply our approach to both synthetic dMRI data and 30 diffusion tensor images from the MIDAS database [5]. The tensor images are interpolated up to 1 mm isotropic resolution using the approach described in [12]. Fiber ODFs are estimated from the tensor data by first scaling the diffusion tensors as in [14], then computing the ODF of the scaled tensors as is done in [12].

For comparison purposes, we generate results using three different algorithms:

- The minimal path approach presented in [12, 20]. This tractography algorithm uses Dijkstra's algorithm on the same graph formulation we present here. This algorithm does not incorporate competition.
- Our proposed random walker tractography algorithm without competition. The algorithm is run for each seed region and background region pair separately. Results from this approach are used to isolate the differences between our algorithm and the minimal path tractography algorithms from [12, 20].
- Our proposed random walker tractography algorithm with competition. We run our algorithm with all seed regions and the background region simultaneously. We use this algorithm to assess the effect of competition to tractography.

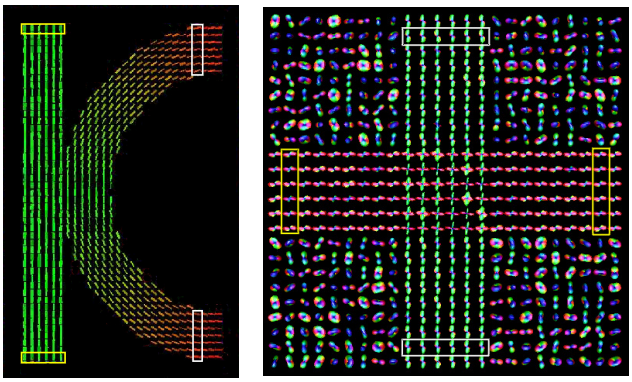

(a) Kissing Fibers (b) Crossing Fibers

Figure 1. Synthetic dMRI phantoms showing complex fiber relationships of kissing and crossing fibers. These two phantoms are used in our tractography experiments with the competing seed regions delineated by white and yellow boxes respectively.

Voxels with fractional anisotropy less than 0.15 are used to define the background region. This threshold matches the termination criteria seen in existing tractography algorithms [1, 3, 9].

3.1. Synthetic dMRI Data

Figure 1 shows two synthetic examples motivating the use of seed region competition in tractography. Both the dMRI with kissing vertical and c-shaped fibers as well as the image with the crossing fibers contain regions where two fiber tracts may compete for space. The corresponding fibers are represented by the seed regions shown in yellow and white respectively. Rician noise was added to the corresponding diffusion weighted images to obtain images with signal-to-noise ratios of 23.74 dB (kissing phantom) and 23.33 dB (crossing phantom) respectively. We hypothesize that the use of competition will reduce the chances of detecting erroneous connections. This hypothesis will be validated if lower connection probabilities are observed within the unseeded tracts.

Figure 2 shows the tractograms corresponding to the seed regions in the vertical tracts for the three different tractography algorithms listed earlier. Note that the minimal path tractography results in Figure 2(a) show high connection probabilities in the unseeded (curved and horizontal) tracts. Further, the connection probabilities do not vary smoothly with respect to the underlying fiber structure. This can be seen in the crossing region in Figure 2(a). Additional non-zero connection probabilities are also seen in the background regions, which demonstrate a lack of coherent connectivity. This noise in the tractograms stems from com-

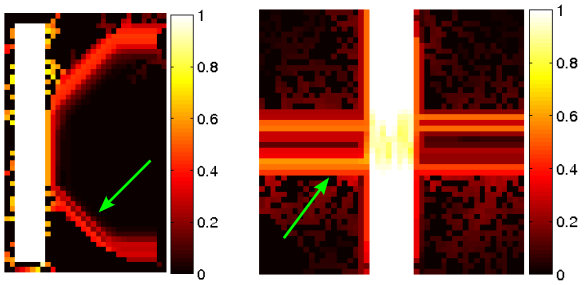

(a) Minimum Path [20]

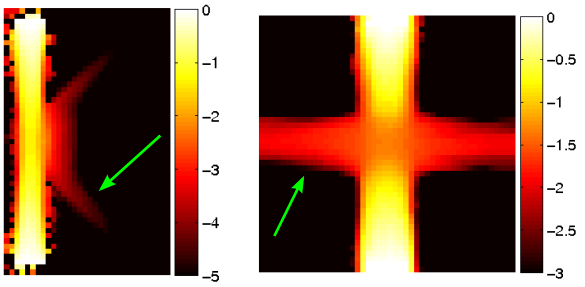

(b) Proposed (without competition)

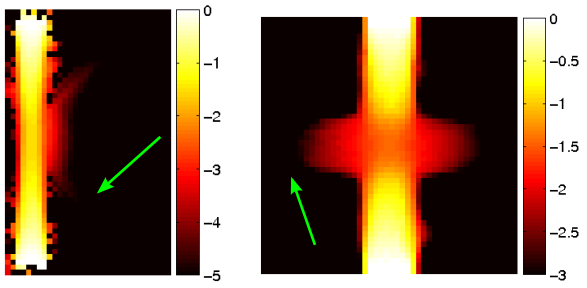

(c) Proposed (with competition)

Figure 2. Tractography results for the crossing and kissing fiber phantoms. Note that our approach in (b) and (c) produces smoother tractograms than the minimal path approach in (a) as we avoid local computation of the connection probabilities. Further, the introduction of competition reduces the chances of tract jumping as shown by the decreasing probability we see away from the seeded vertical tracts. This result is highlighted by the green arrows.

puting connection probabilities based solely on local information.

Figure 2(b) displays the results of our algorithm without competition. Note that, like probabilistic tractography algorithms shown in [3, 9], our connection probabilities decrease as a function of distance and are therefore analyzed in logarithmic scale. Even in logarithmic scale, we see a decrease in tract jumping in the unseeded tract. We also see a smoother spatial distribution in connection probabilities. These differences are due to the computation of all connection probabilities through the closed-form solution to (7). Similar results were seen for the seeded curved and horizontal tracts.

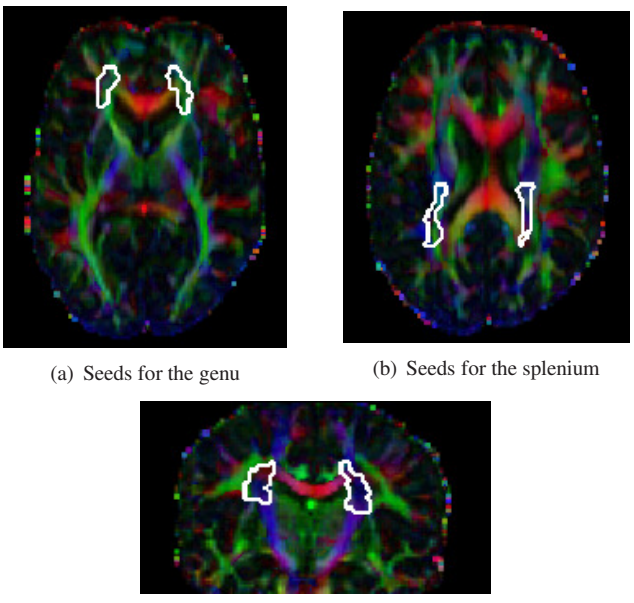

(a) Seeds for the genu

(b) Seeds for the splenium

(c) Seeds for the corpus callosum body

Figure 3. Seed regions defined for examining the strength of the tracts passing through different regions of the Corpus Callosum (CC). These seed regions are chosen within the crossing region between the CC and the internal capsule in order to test the effect that the competing seeds within the internal capsule have on connections within the CC.

Figure 2(c) displays the tractograms from our algorithm with competition. Note that, as hypothesized, the competition further reduces the connection probabilities within the unseeded tract. For the kissing phantom, the connection probabilities in the unseeded curved tract decrease by an average (over the tract) of 42.80% with the addition of competition. The crossing phantom shows a similar decrease in connection probabilities in the unseeded, horizontal tract (48.57%). Simiar results were again seen with the seeded curved and horizontal tracts. These results support the hypothesis that spatial competition in a tractography algorithm reduces the generation of erroneous connections.

3.2. Real dMRI Data

To test the effect of our competition-based tractography on real data, we set up an experiment to examine the different sections of the corpus callosum (CC): the Genu, the Splenium, and the CC Body. For 30 diffusion MRI scans from the MIDAS database [5], we place seed regions in the anterior, middle, and posterior regions of the internal capsule where the internal capsule crosses with the CC as shown in Figure 3. The seed regions are mapped from the LONI ICBM DTI-81 atlas [17] using DT-REFinD deformable registration [19]. These seed regions were chosen to test the effect competing seed regions have in restricting connections through the internal capsule to different sec-

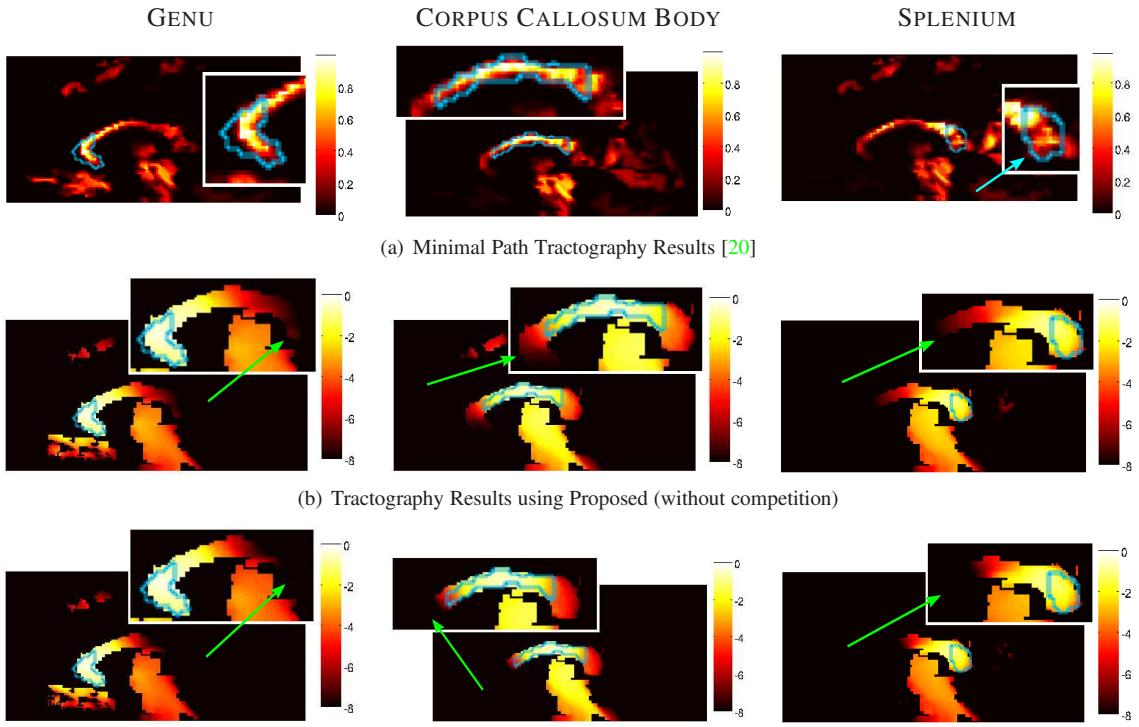

(a) Minimal Path Tractography Results [20]

(b) Tractography Results using Proposed (without competition)

(c) Tractography Results using Proposed (with competition)

Figure 4. Tractography results near the mid-saggital plane for the seed regions in Figure 3. The different sections of the Corpus Callosum (CC) are delineated in blue using atlas-based segmentation. Tractography results within the CC are scaled up and shown in insets. Note that the connection probabilities for the minimal path approach in (a) are noisy as a result of their local computation. An example is pointed out by the blue arrow. Our approach is less susceptible to noise and shows a smoother result. Further, note that the addition of competition reduces the connection probabilities outside the seeded sections of the CC, as shown by the darker regions highlighted by the green arrows.

tions of the CC. We hypothesize that the Genu, CC Body, and Splenium would be most strongly connected to the anterior, middle, and posterior regions of the internal capsule respectively. We further hypothesize that adding competition will reduce the connection probabilities in the unseeded sections of the CC.

Figure 4 shows a representative example of the tractograms generated near the mid-saggital plane for the given seed regions. Shown in Figure 4(a) are the tractograms for the minimal path approach in [12, 20]. These results show the effect imaging noise has on the computed connection probabilities. The connections probabilities vary erratically within the CC due to their local computation, as highlighted in the splenium by the blue arrow.

Figures 4(b) and 4(c) display the tractograms from our proposed approach without and with competition respectively. Note that our tractograms are smoother and that the different sections of the CC show more homogeneous connection probabilities than in the minimal path tractography results. Again, this stems from computing the connection probabilities through the closed-form solution to (7). Further, the results with competition show sharper tractograms than seen without competition as highlighted by the green arrows in the CC body and splenium. These results imply less erroneous connectivity for the different sections of the CC.

To further investigate the connectivity detected by the three tractography algorithms, we compute the marginal probabilities of each tractogram (*i.e.,* the probabilities of each tractogram divided by the sum of all three tractogram probabilities). For the proposed approach, we follow the convention established in [9] and analyze the max-min normalized log-probabilities. These marginal probabilities capture how well the algorithms can differentiate between the connections of different sections of the CC. Figure 5 displays the resulting marginal probabilities. Note that in all cases, our competitive approach gives the highest marginal probabilities. In all cases, a Kruskal-Wallis test shows these results to be statistically significant with p-values of 2.61×10^{-6}, 4.62×10^{-8}, and 2.28×10^{-6} for the Genu, CC Body, and Splenium respectively. These results support our hypothesis that the addition of competition into tractography improves the quality of the connectivity patterns we compute.

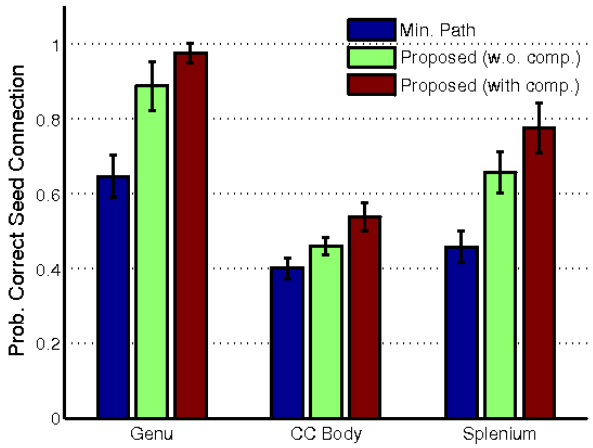

Figure 5. Marginal probabilities within the different sections of the Corpus Callosum with respect to the three seed regions displayed in Figure 3. Note that our approach with competition shows the highest marginal connection probabilities, reflecting improved localization of different sections of the Corpus Callosum.

4. Conclusion

We presented herein a multi-region tractography approach that allows for the incorporation of competition between multiple seeded regions. Our approach generates connection probabilities through a closed-form solution that ensures repeatability of the results. Further, we are able to incorporate knowledge into our tractography algorithm that is beyond the local scale at which most current tractography algorithms operate. Results of our algorithm on thirty adult brain dMRI from the MIDAS database show greater homogeneity in the tractograms of various fiber tracts by avoiding local computation of connection probabilities. We further show that incorporating competition into the tractography process improves the localization of fiber tracts and reduces connectivity to competing tracts. Future work will focus on including non-local information such as region-based [10] or shape-based [18] tract properties into our algorithm's graph formulation.

References

[1] P. J. Basser, S. Pajevic, C. Pierpaoli, J. Duda, and A. Aldroubi. In vivo fiber tractography using DT-MRI data. *Magnetic Resonance in Medicine*, 44:625–632, 2000. 73, 75

[2] C. Beaulieu. The basis of anisotropic water diffusion in the nervous system - a technical review. *NMR in Biomedicine*, 15:435–455, 2002. 73

[3] T. Behrens, M. Woolrich, M. Jenkinson, H. Johansen-Berg, R. Nunes, S. Clare, P. Matthews, J. Brady, and S. Smith. Characterization and propagation of uncertainty in diffusion-weighted MR imaging. *Magnetic Resonance in Medicine*, 50:1077–1088, 2003. 73, 75, 76

[4] B. G. Booth and G. Hamarneh. Exact integration of diffusion orientation distribution functions for graph-based diffusion MRI analysis. In *Proc. of ISBI*, pages 935–938, 2011. 74

[5] E. Bullitt, J. Smith, and W. Lin. Designed database of MR brain images of healthy volunteers. http://www.insight-journal.org/midas/community/view/21. 74, 75, 76

[6] J. Campbell, K. Siddiqi, V. Rymar, A. Sadikot, and G. B. Pike. Flow-based fiber tracking with diffusion tensor and q-ball data: Validation and comparison to principal diffusion direction techniques. *NeuroImage*, 27:725–736, 2005. 73

[7] M. Descoteaux, R. Deriche, T. R. Knösche, and A. Anwander. Deterministic and probabilistic tractography based on complex fibre orientation distributions. *IEEE Trans. Med. Imag.*, 28(2):269–286, 2009. 74

[8] P. Fillard, C. Poupon, and J.-F. Mangin. A novel global tractography algorithm based on an adaptive spin glass model. In *Proc. of MICCAI*, pages 927–934, 2009. 73

[9] O. Friman, G. Farneback, and C.-F. Westin. A Bayesian approach for stochastic white matter tractography. *IEEE Trans. Med. Imag.*, 25(8):965–978, 2006. 73, 75, 76, 77

[10] L. Grady. Multilabel random walker image segmentation using prior models. In *Proc. CVPR*, pages 763–770, 2005. 78

[11] L. Grady. Random walks for image segmentation. *IEEE Transactions on Pattern Analysis and Machine Intelligence*, 28(11):1768–1783, November 2006. 73, 74, 75

[12] Y. Iturria-Medina, E. Canales-Rodríguez, L. Melie-García, P. Valdés-Hernández, E. Martínez-Montes, Y. Alemán-Gómez, and J. Sánchez-Bornot. Characterizing brain anatomical connections using diffusion weighted MRI and graph theory. *NeuroImage*, 36:645–660, 2007. 73, 74, 75, 77

[13] N. Kang, J. Zhang, E. S. Carlson, and D. Gembris. White matter fiber tractography via anisotropic diffusion simulation in the human brain. *IEEE Trans. Med. Imag.*, 24(9):1127–1137, 2005. 73

[14] M. A. Koch, D. G. Norris, and M. Hund-Georgiadis. An investigation of functional and anatomical connectivity using MRI. *NeuroImage*, 16:241–250, 2002. 75

[15] S. Mori, B. J. Crain, V. Chacko, and P. C. van Zijl. Three-dimensional tracking of axonal projections in the brain by magnetic resonance imaging. *Annals of Neurology*, 45(2):265–269, 1999. 73, 75

[16] S. Mori and P. C. van Zijl. Fiber tracking: principles and strategies - a technical review. *Nuclear Magnetic Resonance in Biomedicine*, 15:468–480, 2002. 73

[17] U. L. of Neural Imaging. ICBM DTI-81 atlas. http://www.loni.ucla.edu/Atlases, February 2009. 76

[18] O. Veksler. Star shape prior for graph-cut image segmentation. In *Proceedings of ECCV*, pages 454–467, 2008. 78

[19] B. T. Yeo, T. Vercauteren, P. Fillard, J.-M. Peyrat, X. Pennec, P. Golland, N. Ayache, and O. Clatz. DT-REFinD: Diffusion tensor registration with exact finite-strain differential. *IEEE Transactions on Medical Imaging*, 28:1914–1928, 2009. 76

[20] A. Zalesky. DT-MRI fiber tracking: A shortest paths approach. *IEEE Trans. Med. Imag.*, 27(10):1458–1571, 2008. 73, 75, 76, 77